

Major depressive disorder: early detection using deep learning and pupil diameter

Islam Ismail Mohamed¹, Mohamed Tarek El-Wakad², Khaled Abbas Shafie³, Mohamed A. Aboamer⁴,
Nader A. Rahman Mohamed⁵

¹Department of Biomedical Engineering, Higher Technological Institute, 10th Ramadan City, Egypt

²Department of Biomedical Engineering, Faculty of Engineering and Technology, Future University, New Cairo, Egypt

³Department of Electronics and Communication, Higher Technological Institute, 10th Ramadan City, Egypt

⁴Department of Medical Equipment Technology, College of Applied Medical Sciences, Majmaah University,
Majmaah, Saudi Arabia

⁵Department of Biomedical Engineering, Faculty of Engineering, Misr University for Science and Technology (MUST),
Giza, Egypt

Article Info

Article history:

Received Feb 6, 2024

Revised Apr 8, 2024

Accepted Apr 13, 2024

Keywords:

Convolutional neural networks

Depression early detection

Machine learning techniques

Major depressive disorder

Pupillometric recordings

ABSTRACT

Major depressive disorder stands as a highly prevalent mental disorder on a global scale. Detecting depression at its early stages holds paramount importance for effective treatment. However, due to the coexistence of depression with other conditions and the subjective nature of diagnosis, early identification poses a significant challenge. In recent times, machine learning techniques have emerged as valuable tools for the development of automated depression estimation systems, aiding in the diagnostic process. In this particular study, a deep learning approach utilizing pupil diameter was employed to distinguish between individuals diagnosed with depression and those who are considered mentally healthy. Pupillometric recordings were collected from a total of 58 individuals, comprising 29 healthy individuals and 29 individuals diagnosed with depression. Pupil size was recorded every 4 ms. The performance of three pretrained convolutional neural networks (GoogLeNet, SqueezeNet, and AlexNet) was evaluated for depression classification using the pupil size data. The highest accuracy of 98.28% was obtained with AlexNet. This finding highlights the potential of utilizing pupil diameter as a reliable indicator for objectively measuring depression.

This is an open access article under the [CC BY-SA](https://creativecommons.org/licenses/by-sa/4.0/) license.



Corresponding Author:

Nader A. Rahman Mohamed

Department of Biomedical Engineering, Faculty of Engineering

Misr University for Science and Technology (MUST)

Giza, Egypt

Email: nader.shaaban@must.edu.eg

1. INTRODUCTION

Depression is a pervasive mental health disorder characterized by persistent feelings of sadness, hopelessness, and loss of interest or pleasure in activities. It is a serious mental illness that has significant effects on individuals, their families, and communities. According to the World Health Organization (WHO), it is projected that by the year 2030, depression will be recognized as the most widespread mental disorder [1]. Severe cases of depression have the potential to lead to suicide, with approximately 50% of suicides linked to depression [2]. With its significant impact on individuals' quality of life and functioning, accurate and timely diagnosis of depression is crucial for effective treatment and management. Traditional diagnostic methods often rely on subjective self-reporting or clinician-administered questionnaires, which may be influenced by

various factors such as social desirability or recall bias. In recent years, there has been growing interest in exploring objective physiological markers for diagnosing depression, among which pupil diameter has emerged as a promising candidate.

The aim of this study is to explore the potential of using deep convolutional neural networks (DCNNs) to detect depression through the analysis of signals derived from pupil diameter. By leveraging advancements in computational methods and deep learning, this study achieved high accuracy in the classification of depression based on pupil diameter data. The study will investigate the feasibility of pupil diameter as a diagnostic tool, aiming to surpass the accuracy thresholds achieved by existing methods. Through this research, we aim to contribute to the field of depression detection and offer insights into the effectiveness of utilizing pupil diameter-related signals for diagnostic purposes.

Literature review and related work. The pupil, the aperture in the center of the iris, plays a crucial role in regulating the amount of light entering the eye. However, research has shown that pupil diameter is also modulated by cognitive and emotional processes. It is well-established that both the parasympathetic and sympathetic branches of the autonomic nervous system regulate the pupil's diameter response. Changes in pupil size over time have become a reliable clinical indicator for assessing autonomic nervous system function. Pupillary response is frequently employed as a diagnostic tool to identify imbalances in the autonomic nervous system [1], [2].

Changes in pupil size have been linked to arousal, attention, cognitive load, and emotional valence. For instance, increased pupil dilation is associated with heightened emotional arousal or cognitive effort, while constriction may reflect reduced arousal or cognitive processing. The measurement of pupil diameter appears to offer distinct and valuable insights into the cognitive processes of the human mind. The pupillary system has garnered considerable interest in psychophysiological studies for many centuries [3]. Pupil size is known to undergo changes in response to emotional arousal and cognitive demand, as evidenced by studies conducted by [4]–[6]. Historically, pupil size fluctuations have been studied in relation to sleepiness or cognitive load, rather than for gathering information about the autonomic nervous system [7], [8].

Hosseinfard *et al.* [9] explored the efficacy of nonlinear electroencephalography (EEG) analysis for distinguishing between depressed patients and healthy individuals, utilizing 45 unmedicated depressed participants and 45 controls. Employing techniques like detrended fluctuation analysis. The study applies k-nearest neighbor (KNN), linear discriminant analysis (LDA), and logistic regression (LR) classifiers, the study achieves up to 90% accuracy in classification by combining nonlinear features, significantly outperforming single-feature approaches. The findings suggest that nonlinear EEG metrics can effectively complement traditional diagnostic methods for depression, offering a promising tool for early detection and intervention.

Moreover, research by Siegle *et al.* [10] demonstrated differences in baseline pupil diameter between depressed and non-depressed individuals. The research found that depressed participants exhibited a mean baseline pupil diameter of 3.5 mm, whereas non-depressed individuals had a mean baseline pupil diameter of 4.0 mm. The research reported a statistically significant difference in baseline pupil diameter between depressed and non-depressed participants, with an effect size of $d = 0.8$ ($p < 0.01$). This indicates a large and statistically significant difference in pupil diameter between the two groups, supporting the accuracy of baseline pupil diameter as a biomarker for depression.

Schumann *et al.* [11] investigated the link between pupil diameter and depression in individuals with major depression. Alongside cardiovascular dysregulation, their findings demonstrated that individuals with major depression (MD) exhibited autonomic imbalance as indicated by their pupil diameters. The sympathetic and parasympathetic nervous systems both influence pupil size. This study aimed to identify signs of autonomic dysfunction in resting pupillography recordings and ascertain how these indicators relate to cardiovascular system functioning [11].

The investigation encompassed pupillographic parameters such as baroreflex sensitivity (BRS), pupillary unrest index (PUI), root mean square of successive heartbeat intervals, mean pupil diameter (DIA), LF/HF (ratio of low and high-frequency power of pupil size fluctuations), with “r” and “l” subscripts denoting right and left pupil, and heart rate (HR) [11]. The findings indicated significantly increased restlessness and mean pupil widths in patients with depression [11]. These patients exhibited larger pupil diameters and higher abnormal values. An increase was noted in both their low-frequency component and total spectral power for frequencies ranging from 0.01 to 0.5 Hz. Conversely, high-frequency power and the low-to-high frequency ratio did not exhibit significant increases. A strong correlation was observed between the mean diameter, unrest index of the left pupil, and the level of symptom severity measured by beck's depression inventory [11].

Li *et al.* [12] employed deep learning techniques, incorporating a novel cascade parallel multi-scale residual module for analyzing pupil wave data. In contrast to the cascade network VGGNet13, the parallel multi-scale module Inception, HS-ResNet, and Res2Net, their deep learning module demonstrated superior assessment performance. It achieved a remarkable RMSE of 4.41, suggesting effective integration of diverse

multi-scale information into the model. Leveraging pupil wave data, the model acquired a broader range of features associated with the representation of depression and anxiety states.

Ding *et al.* [13] conducted a study to classify major depressive disorder (MDD) patients and healthy controls using EEG data. The study included 144 individuals with MDD and 204 healthy controls matched to them. Participants observed emotional and neutral stimuli while low-cost, portable devices recorded their EEG, eye tracking data, and galvanic skin reaction.

The binary classification model was built by training three machine learning algorithms: random forests (RF), LR, and support vector machine (SVM). LR yielded the best classification F1-score, achieving an accuracy of 79.63%, precision of 76.67%, recall of 85.19%, and an F1-score of 80.70%. The study had limitations such as the inclusion of only outpatient participants and the absence of older patients [13]. Nonetheless, the machine learning approach proved valuable for classifying MDD patients and healthy controls, potentially aiding diagnostic processes.

Mumtaz and Qayyum [14] developed two deep learning architectures a one-dimensional convolutional neural network (1DCNN) and a hybrid model combining 1DCNN with long short-term memory (LSTM). Their aim was to classify depressed individuals and healthy controls using EEG data. The models were trained and evaluated on resting-state EEG data from 33 depressed patients and 30 healthy controls. The CNN model achieved an impressive accuracy of 98.32%, indicating its potential for accurately distinguishing between the two groups. Mumtaz and Qayyum [14] research underscore the effectiveness of deep learning approaches in leveraging EEG data for depression classification.

Sandheep *et al.* [15] conducted a study on depression classification using EEG signals. They employed a CNN as a machine learning approach and trained the model on EEG data from 30 depressed individuals and 30 normal controls. The CNN achieved remarkable results, achieving an accuracy of 99.31% for classifying depression based on EEG signals from the right hemisphere of the brain and 96.3% using signals from the left hemisphere [15]. This research highlights the efficacy of the CNN method in accurately identifying depression through EEG data.

Zhu *et al.* [16] explored the fusion of EEG and pupil area signals to develop a practical and efficient model for mild depression recognition. They introduced a novel approach called the mutual information based fusion model (MIBFM), which utilized pupil area signals to select EEG electrodes using mutual information. The proposed MIBFM achieved the highest accuracy of 87.03%.

Schultebrucks *et al.* [17] employed a deep neural network to extract facial features, speech prosody, movement parameters (e.g., pupil dilation), and natural language content to classify individuals with MDD. Both video and audio markers significantly contributed to accurate classification. The algorithm achieved an AUC of 0.86.

Zhu *et al.* [18] investigated the potential of early depression detection through time-frequency analysis of internet behaviors. Utilizing classification and prediction models, they aimed to differentiate and identify individuals' mental states. They employed z-score normalization to ensure reliable results, standardizing features extracted from internet behaviors for meaningful comparisons. Their approach, utilizing the Naive Bayes algorithm, achieved a precision rate of 76.8%.

Schumann *et al.* [19] delved into the relationship between pupil diameter fluctuations and respiratory and cardiovascular rhythms. Analyzing pupil diameters from 29 individuals, they observed distinct lateralization in pupil unrest. To mitigate the impact of eye blinks, they employed a median filter with a 600 ms time window followed by temporal smoothing of 200 ms. The correlation with vagal heart rate regulation and baroreflex sensitivity underscores the significance of the left pupil's fluctuations in assessing autonomic nervous system status.

Kramarić *et al.* [20] implemented heart rate variability (HRV) analysis as a marker for acute stress in newborns. Receiver operating characteristic (ROC) curve analysis was used to evaluate the diagnostic properties of HRV indices, demonstrating their potential as clinical markers. The indices achieved an accuracy of 87.5%, with polynomial detrending used to eliminate signal trends. This study highlights HRV analysis potential in newborns for assessing acute stress.

Kang *et al.* [21] utilized Welch's periodogram to analyze EEG signals for depression detection. They generated asymmetry images by calculating relative powers across different frequency bands and employed them as inputs in a CNN. Impressively, the CNN trained on these images achieved an accuracy of 98.85% in accurately detecting depression [21]. The Table 1 presents a summary of the outcomes obtained from the studies approaches described earlier. It highlights the exceptional results of our research in comparison to those of others.

Problem statement: considering the findings of prior studies, few investigations have focused on pupil diameter as a differentiator between normal and depressed cases. In contrast, a significant number of studies have concentrated on EEG signals as an effective method to distinguish between normal and depressed cases. Although literature suggests that pupil diameter shows promise as a potential biomarker for

diagnosing depression, and it revealed some studies that have consistently demonstrated differences in pupillary responses between depressed and non-depressed individuals, highlighting the potential utility of pupillometry in clinical settings.

However, further research is needed to validate the reliability and specificity of pupillary measures for depression diagnosis. Also, while the most accurate results have been obtained using pupil area [16], not exceeding 90%, the potential of pupil diameter as a diagnostic tool for distinguishing between normal and depressed patients remains promising. Furthermore, computational methods hold substantial promise for advancing our understanding of psychiatric disorders, offering benefits in terms of diagnosis speed and accuracy compared to traditional approaches. This paper introduces a new approach for detecting depression by harnessing the power of DCNNs and analyzing pupil diameter-derived signals with high accuracy.

Table 1. A summary of the outcomes obtained from the studies

Researcher	AI	Learning model	Dataset	Result
Our research	Deep learning	GoogLeNet, SqueezeNet, AlexNet	Pupil diameter	98.28%
Behshad <i>et al.</i> [9]	Machine learning	KNN, LDA, LR	EEG	90%
Ding <i>et al.</i> [13]	Machine learning	RF, LR, SVM	EEG, eye tracking, galvanic skin reaction	79.63%
Mumtaz <i>et al.</i> [14]	Deep learning	1DCNN, LSTM	EEG	98.32%
Sandheep <i>et al.</i> [15]	Deep learning	CNN	EEG	99.31%
Zhu <i>et al.</i> [16]	Machine learning	Mutual information based fusion model (MIBFM)	EEG, Pupil area	87.03%
Schultebrucks <i>et al.</i> [17]	Deep learning	Deep neural network	Facial features, speech prosody, Movement parameters	AUC of 0.86
Zhu <i>et al.</i> [18]	Machine learning	Naive Bayes	Internet behaviors	Precision rate: 76.8%
Kramarić <i>et al.</i> [20]	Machine learning	ROC curve analysis	HRV	87.5%
Kang <i>et al.</i> [21]	Deep learning	CNN	EEG	98.85%

2. METHOD

2.1. Method and data collection

In this research paper, we utilized a previously published dataset that investigated the interrelation of cardiovascular dysfunction and pupillary fluctuations in patients with major depression [11]. The MP150 polygraph from BIOPAC systems Inc. in Goleta, CA, USA was employed to conduct cardiovascular and pupillometric recordings on a group of participants. The study involved two groups: 29 unmedicated individuals diagnosed with major depression (21 females, 8 males, mean age: 37.8 ± 12.2 , mean BMI: 23.8 ± 4.1) and a control group of 29 healthy individuals (21 females, 8 males, mean age: 36.9 ± 12.5 , mean BMI: 23.5 ± 4.1) [11].

Participants in our study were individuals hospitalized in inpatient wards under the diagnosis of a staff psychiatrist. All participants met the diagnostic criteria for major depressive disorder as outlined in DSM-IV. Importantly, none of these patients had previously received any antidepressant medications before the research. The severity of depressive symptoms was assessed using the Hamilton rating scale for depression.

In line with Hamilton (1960), the study involved interviews with both patients and healthy volunteers to mitigate potential influences from clinical deficits. Additionally, all participants completed Beck's depression assessment, as developed by Beck in 1961. The healthy control group comprised individuals without any current or previous psychiatric, neurological, or clinically relevant illnesses.

All participants provided their informed written consent in accordance with the authorized protocol by the Ethics Committee of Jena. The investigations were conducted during the late afternoon and early evening, specifically between 2:00 pm and 7:00 pm. The examination room maintained a tranquil atmosphere characterized by minimal noise and subdued illumination from a low-intensity ambient light source. Participants wore headphones to minimize ambient noise. A dark gray ellipse served as a fixation anchor, displayed on a monitor above the couch. The ambient temperature was set at 22 °C.

Throughout the 20-minute test, the room remained silent. An indirect light source in the form of a beamer ensured consistent lighting. A 22-inch monitor displayed an ellipse covering the entire screen to facilitate eye movement tracking within the designated pupillometric system area. The initial five-minute period was excluded from analysis to allow participants to acclimate.

Pupil size assessment was conducted at 4-millisecond intervals using the infrared camera system RED 250, manufactured by SensoMotoric Inc. in Boston, MA, USA. The decision to record pupil size at this specific frequency is rooted in the need to capture rapid changes in pupillary responses associated with

emotional processing. The 4ms interval was chosen to ensure a high temporal resolution, and to precisely capture fluctuations in pupil diameter.

2.2. Proposed approach

The proposed approach is structured into two fundamental experiments: the first without data segmentation, and the second with data segmentation. The first experiment consists of four main sections: pre-processing, feature extraction, data partitioning, and classification. In the pre-processing phase, the following steps were applied: normalization, median filter (200 ms), non-linear detrending, and median filter (600 ms). Feature extraction utilized Welch’s periodogram, illustrated in Figure 1. The classification phase involved testing three distinct DCNN models.

The second experiment mirrors the steps of the first experiment, with the addition of data segmentation to expand the dataset from (29 healthy, 29 depressed) cases to (145 healthy, 145 depressed), as depicted in Figure 2. The initial dataset comprises a total of 58 cases, divided equally between healthy and depressed classifications. The dataset encompasses measurements of both right and left pupil diameters. Z-score normalization was applied to standardize the data on a uniform scale.

To eliminate unwanted signal noise, a median filter with window sizes of 200 ms and 600 ms was employed. A 6th order polynomial detrending technique was utilized to remove underlying trends from the signal. For feature extraction, the Welch’s periodogram method was employed. This technique facilitated obtaining the power spectral density for subsequent analysis purposes.

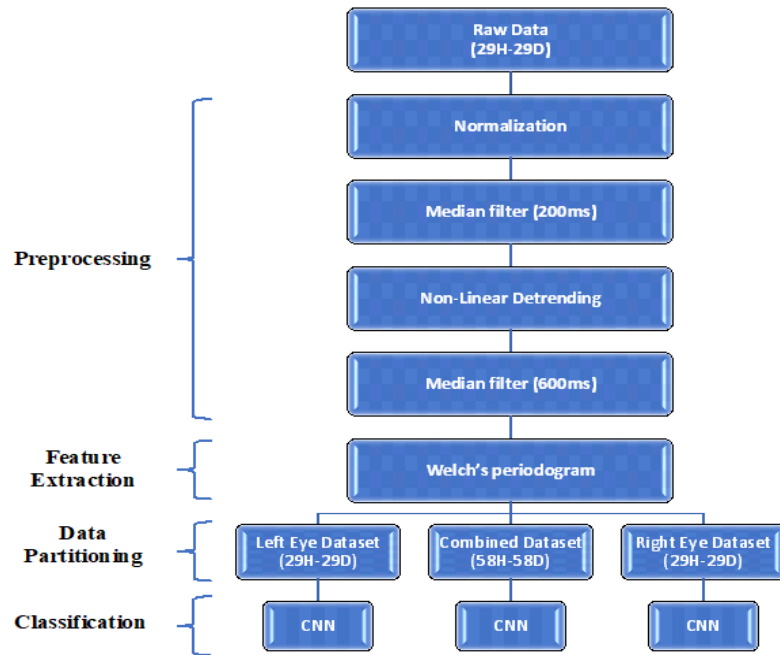


Figure 1. Proposed system (without segmentation)

2.3. Dataset preprocessing

2.3.1. Normalization

Normalization is a crucial step in scientific data analysis, aiming to eliminate unwanted variations and biases. This process enhances the accuracy and reliability of research outcomes. By adjusting data values to a common scale, normalization enables comparability between variables. This, in turn, facilitates effective data integration, allowing for meaningful statistical analysis and interpretation.

In this study, the Z-score normalization technique is employed. For a given value x, the Z-score can be calculated using the (1).

$$z = \frac{x - \mu}{\sigma} \tag{1}$$

Here, x represents a variable, μ stands for the mean of x, and σ denotes the standard deviation of x.

The Z-score quantifies the distance between x and μ , with its magnitude influenced by the standard deviation σ . A negative z value indicates that x is below the mean μ . To ensure uniformity, all data for each individual are normalized using the Z-score method [18]. Figures 3 and 4 illustrate the data before and after normalization. In particular, (a) depicts the left pupil diameter, while (b) showcases the right pupil diameter for both depressed and healthy cases.

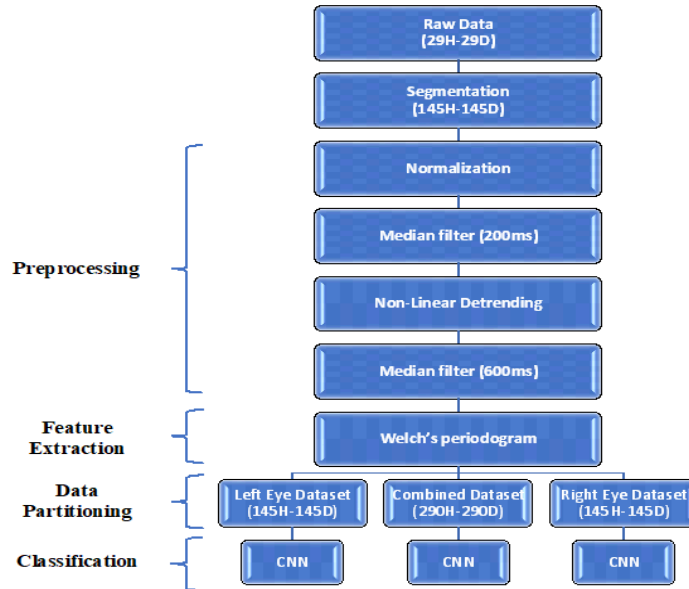


Figure 2. Proposed system (with segmentation)

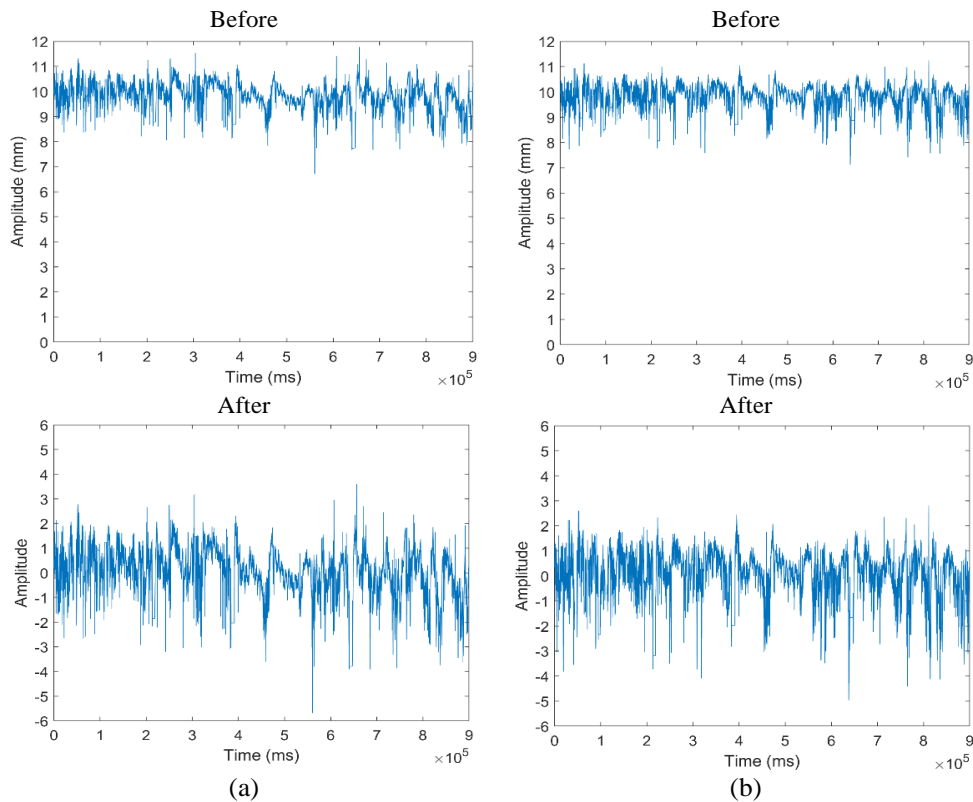


Figure 3. Sample of data before and after normalization (a) for depressed left pupil diameter and (b) for depressed right pupil diameter

Before

Before

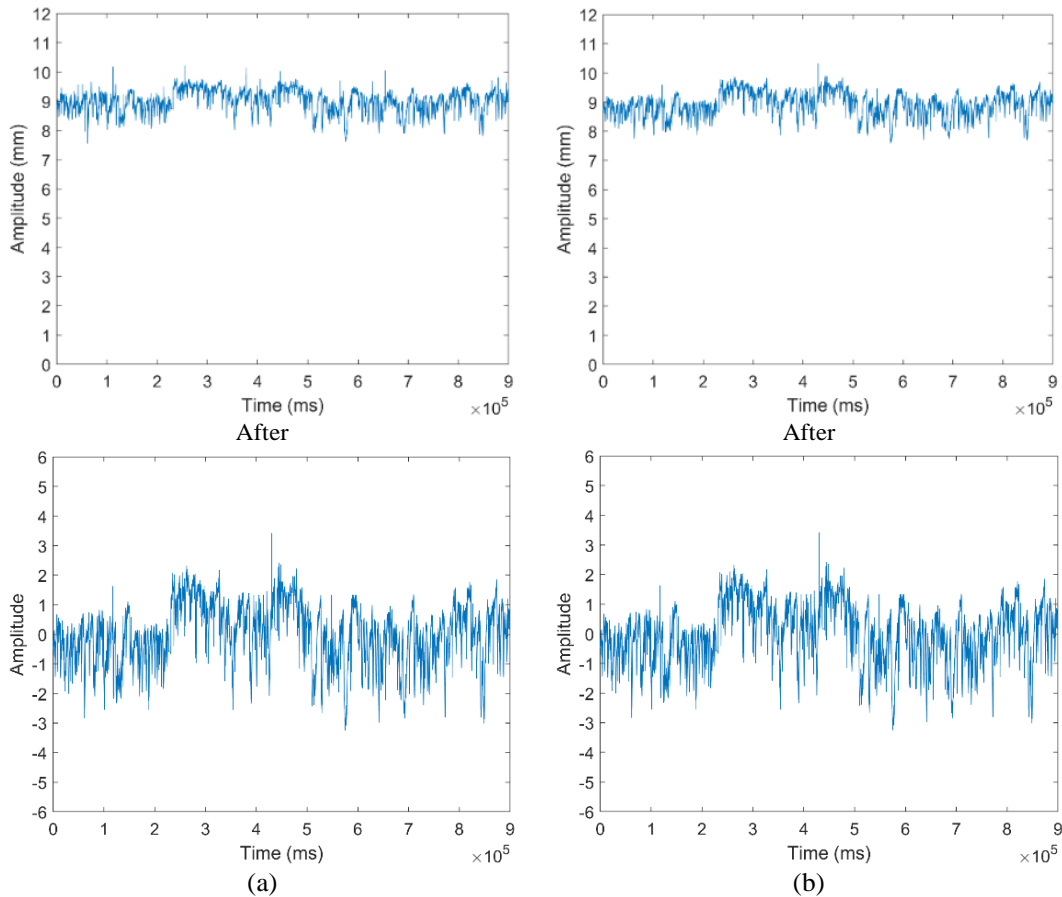


Figure 4. Sample of data before and after normalization (a) for healthy left pupil diameter and (b) for healthy right pupil diameter

2.3.2. Median filtering

The median filter proves to be highly effective in mitigating random noise. This filtering technique involves the movement of a window across the signal. In the context of your study, the median filter serves as a valuable tool for addressing eye blinks, which manifest as sudden drops in pupil diameter. To specifically handle this issue, a median filter with a 600 ms time window is employed subsequent to trend removal. Additionally, a 200 ms time window is utilized for temporal smoothing before the removal of trends. These measures are implemented with the intent of enhancing model accuracy.

Unwanted noise possesses the potential to obscure the pertinent information that the model seeks to grasp during the learning process. Consequently, it becomes imperative to eliminate this unwanted noise. The application of a conventional median filter involves the selection of the median value, often referred to as the midpoint, from a given window. This process aids in preserving the integrity of the valuable data by smoothing out noise and preserving meaningful information.

The median of n observations $x_i, i = 1, \dots, n$ is denoted by $med(x_i)$ and it is given by (2):

$$med(x_i) = \begin{cases} x_{(v+1)} & \text{where } n \text{ is odd, and } n = 2v + 1 \\ \frac{1}{2}(x_{(v)} + x_{(v+1)}) & \text{where } n \text{ is even, and } n = 2v \end{cases} \quad (2)$$

where $x_{(i)}$ denotes the i -th order statistic.

A one-dimensional median filter of size $n = 2v + 1$ is defined through the input-output relation:

$$y_i = med(x_{i-v}, \dots, x_i, \dots, x_{i+v}) \quad i \in Z \quad (3)$$

In (3), the input is the sequence x_i where $i \in Z$, and the output is the sequence y_i where $i \in Z$. This concept is also known as the running median or moving median [22], and it plays a significant role in data processing.

As demonstrated in Figures 5 and 6, the data undergoes a median filter with a 200 ms window. Specifically, (a) pertains to the left pupil diameter, while (b) corresponds to the right pupil diameter for both depressed and healthy cases. The application of the median filter effectively refines the data, contributing to improved signal quality and aiding in the identification of meaningful trends and patterns.

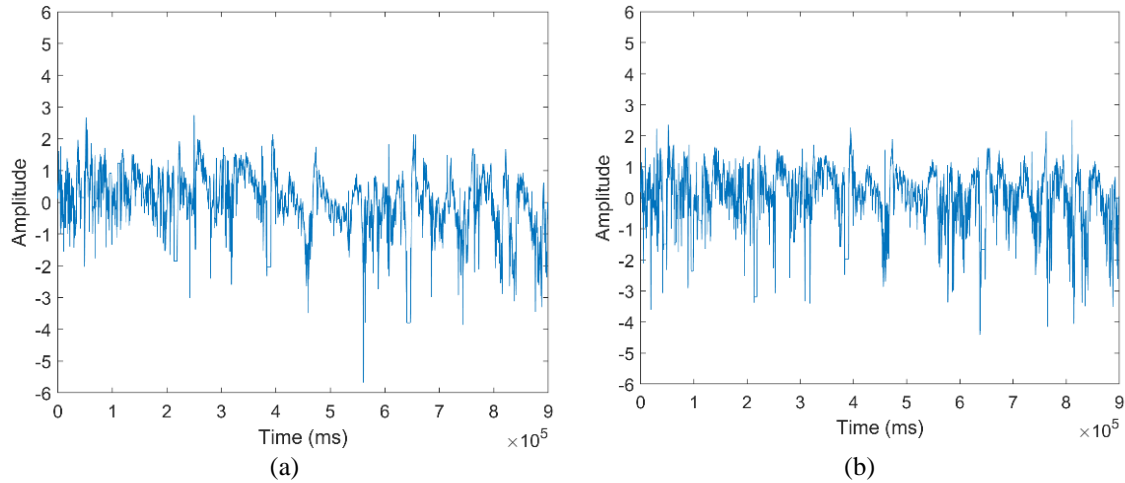


Figure 5. Signal after median filter 200 ms (a) for depressed left pupil diameter and (b) for depressed right pupil diameter

Prior to implementing the 600 ms median filter, a sixth-degree polynomial detrending technique was employed to eliminate any existing trends present in the acquired signal. This detrending process is crucial for removing long-term variations from the signal, allowing subsequent analysis and filtering to focus more accurately on the fluctuations of interest. By applying the sixth-degree polynomial detrending, the data is prepared for further processing, ensuring that the trends are adequately addressed before the median filter is applied. This multi-step approach enhances the quality of the data and contributes to more accurate and meaningful outcomes in the subsequent stages of analysis.

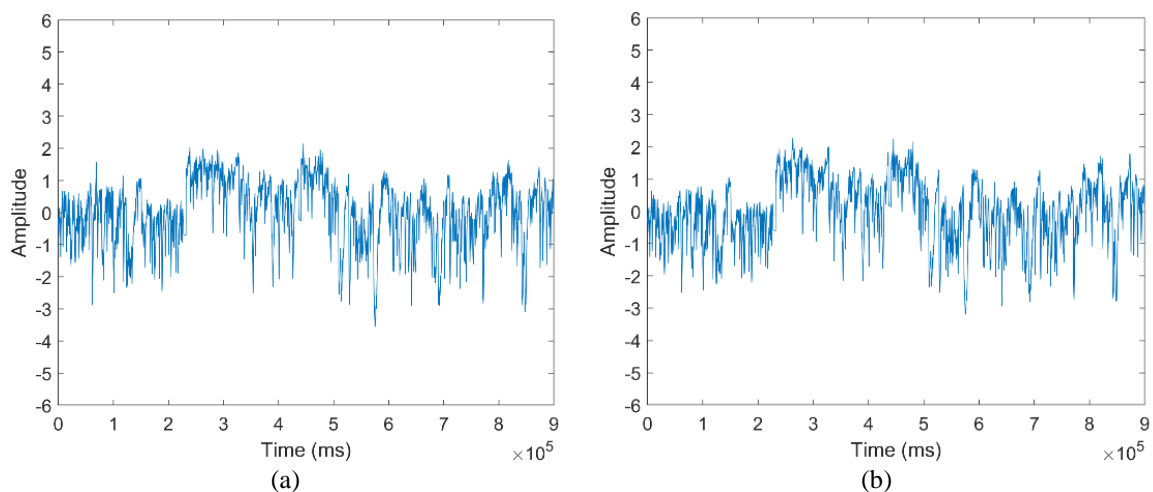


Figure 6. Signal after median filter 200 ms (a) for healthy left pupil diameter and (b) for healthy right pupil diameter

2.3.3. Nonlinear detrending

To execute the nonlinear detrending method, the MATLAB functions “polyfit” and “polyval” were employed. The “polyfit” function calculates the coefficients for a polynomial $p(x)$ of degree n that best fits the data in y [23].

$$p(x) = p_1x^n + p_2x^{n-1} + \dots + p_nx + p_{n+1} \tag{4}$$

The coefficients in p are organized in descending powers, and the length of p is $n + 1$. The vector x represents the query points corresponding to the fitted function values in y . The result y is the fitted values at the query points contained in x . The parameter n signifies the degree of the polynomial fit, determining the power of the left-most coefficient in p .

Subsequently, the “polyval” MATLAB function is employed to evaluate the polynomial p at each point in x , and the obtained polynomial curve is subtracted from the original signal to eradicate trends [24]. In this study, a sixth-order polynomial was fitted to the signal to eliminate nonlinear trends. This approach effectively eliminates trends, resulting in signals that exhibit no remaining baseline shifts. Consequently, these signals are now prepared for further processing and analysis.

As demonstrated in Figures 7 and 8, the data displays the effects of the detrending process. Specifically, (a) pertains to the left pupil diameter, while (b) corresponds to the right pupil diameter for both depressed and healthy cases. The detrending step successfully removes nonlinear trends, setting the stage for subsequent analyses that require trend-free data.

After applying a sixth-degree polynomial detrending, a 600 ms median filter was used to eliminate sudden drops in pupil diameter. As depicted in Figures 9 and 10, the data after applying the 600 ms median filter is presented, with (a) representing the left pupil diameter and (b) representing the right pupil diameter for both depressed and healthy cases, respectively.

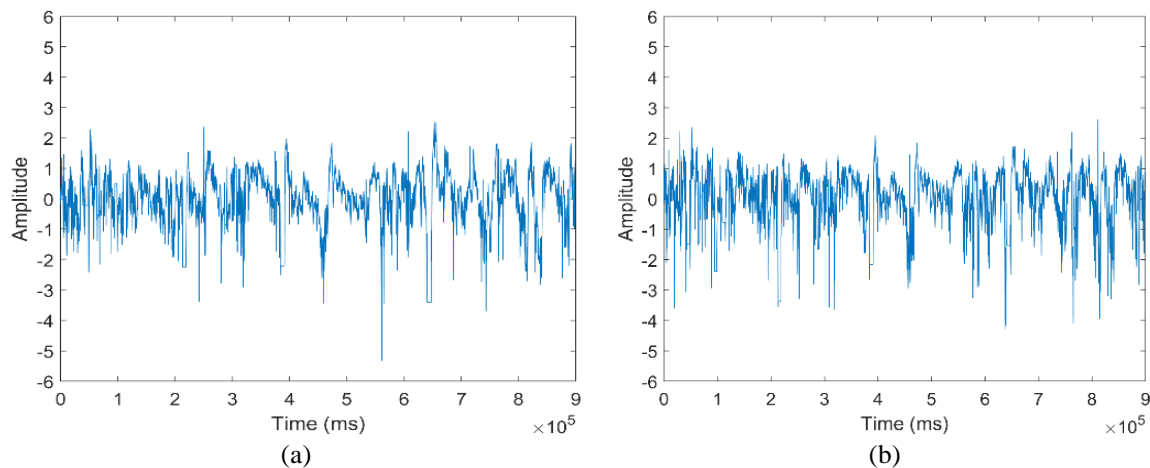


Figure 7. Signal after remove trend (a) for depressed left pupil diameter and (b) for depressed right pupil diameter

2.3.4. Welch’s periodogram

Welch’s method involves using an averaged modified periodogram to estimate the power spectrum. This technique divides the time series into overlapping segments, or windows, and computes the periodogram for each individual window. By averaging these resultant periodograms, the Welch periodogram is derived [25].

Let’s denote the m -th windowed, zero-padded frame from the signal x as $x_m(n)$, which is defined when using the rectangular window $w(n)$ as (5):

$$x_m(n) \triangleq w(n)x(n + mR), n = 0, 1, \dots, M - 1, m = 0, 1, \dots, K - 1 \tag{5}$$

here, R represents the window hop size, and K represents the number of available frames. The periodogram of the m -th block can then be expressed as (6).

$$P_{x_m, M}(w_k) = \frac{1}{M} |FFT_{N, k}(x_m)|^2 \triangleq \frac{1}{M} \left| \sum_{n=0}^{M-1} x_m(n) e^{-j2\pi nk/N} \right|^2 \tag{6}$$

This (7) remains consistent with the earlier representation. The Welch estimate of the power spectral density is obtained through:

$$\hat{S}_x^W(w_k) \triangleq \frac{1}{K} \sum_{m=0}^{K-1} P_{xm,M}(w_k) \tag{7}$$

As illustrated in Figure 11, the data is presented after the application of Welch’s periodogram. In this depiction, Figure 11(a) pertains to depressed subjects, while Figure 11(b) corresponds to healthy subjects, respectively.

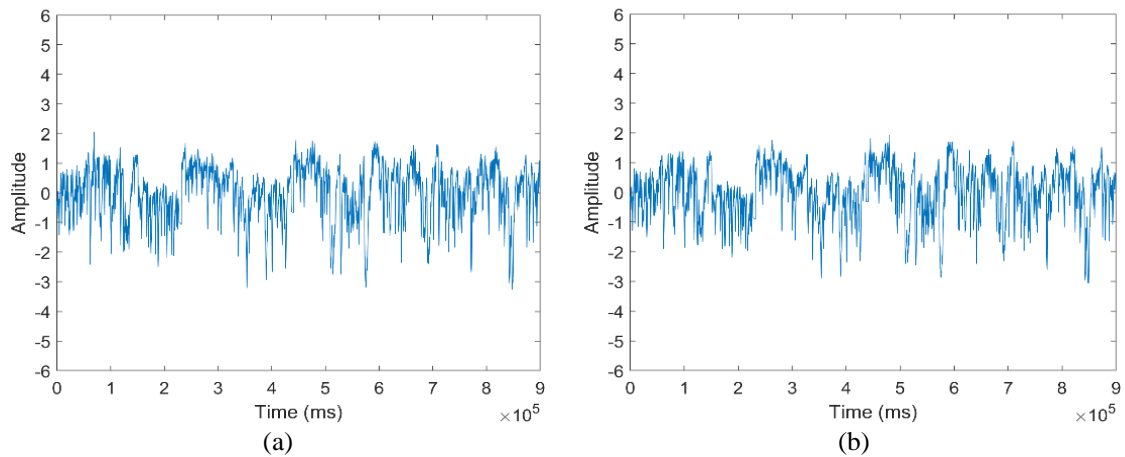


Figure 8. Signal after remove trend (a) for healthy left pupil diameter and (b) for healthy right pupil diameter

2.3.5. Segmentation

The dataset comprises 58 cases, evenly distributed between 29 healthy and 29 depressed cases. Each case encompasses a 15-minute recording of the pupil diameter signal for both the left and right eyes. This dataset has been categorized into three distinct subsets: recordings from the left eye, recordings from the right eye, and a consolidated dataset combining both eyes’ recordings.

In a concerted effort to enhance our dataset and elevate the precision of classification, each case’s signal has been divided into five segments, each spanning a duration of three minutes. This segmentation procedure has effectively augmented the dataset, resulting in a total of 145 cases for both healthy and depressed subjects. Consequently, the combined dataset comprises a total of 290 cases.

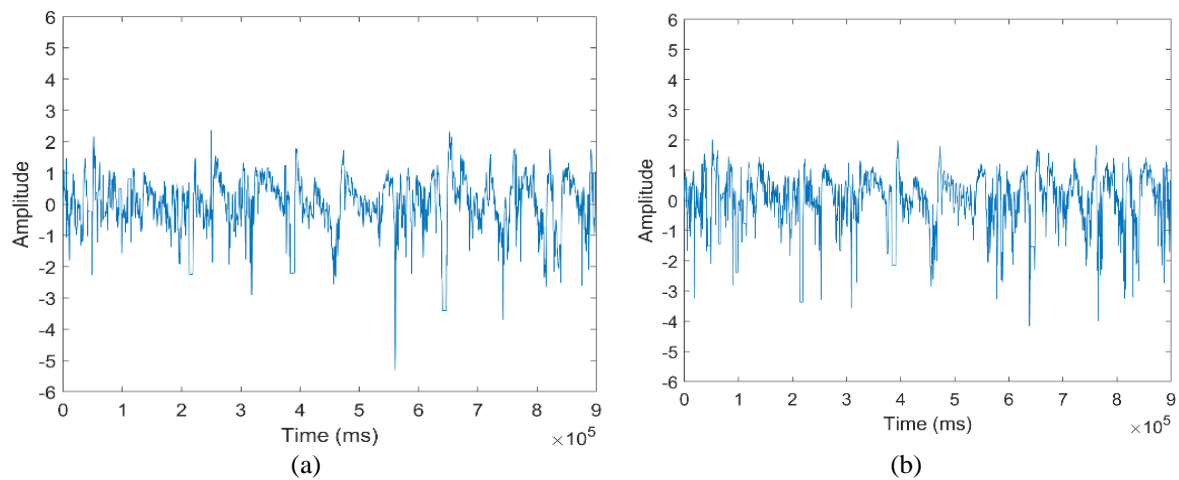


Figure 9. Signal after median filter 600 ms (a) for depressed left pupil diameter and (b) for depressed right pupil diameter

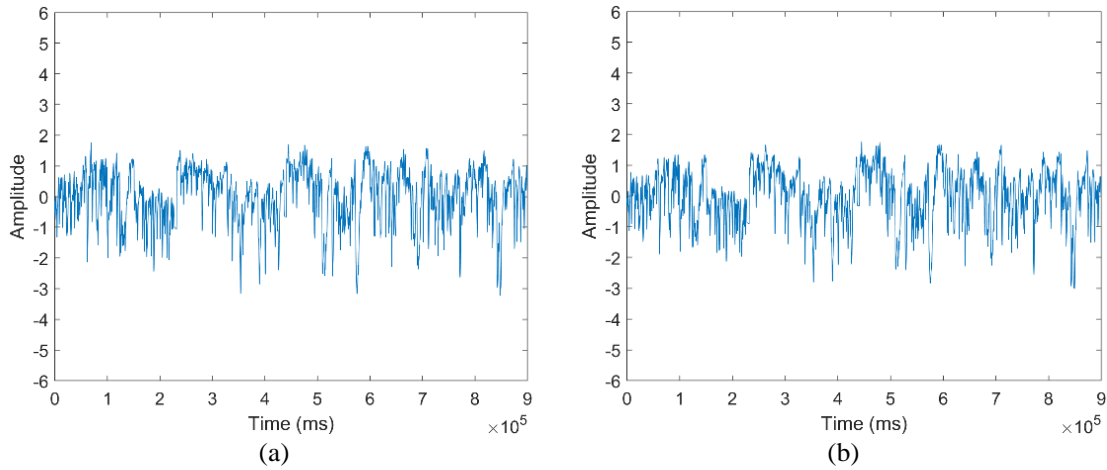


Figure 10. Signal after median filter 600 ms (a) for healthy left pupil diameter and (b) for healthy right pupil diameter

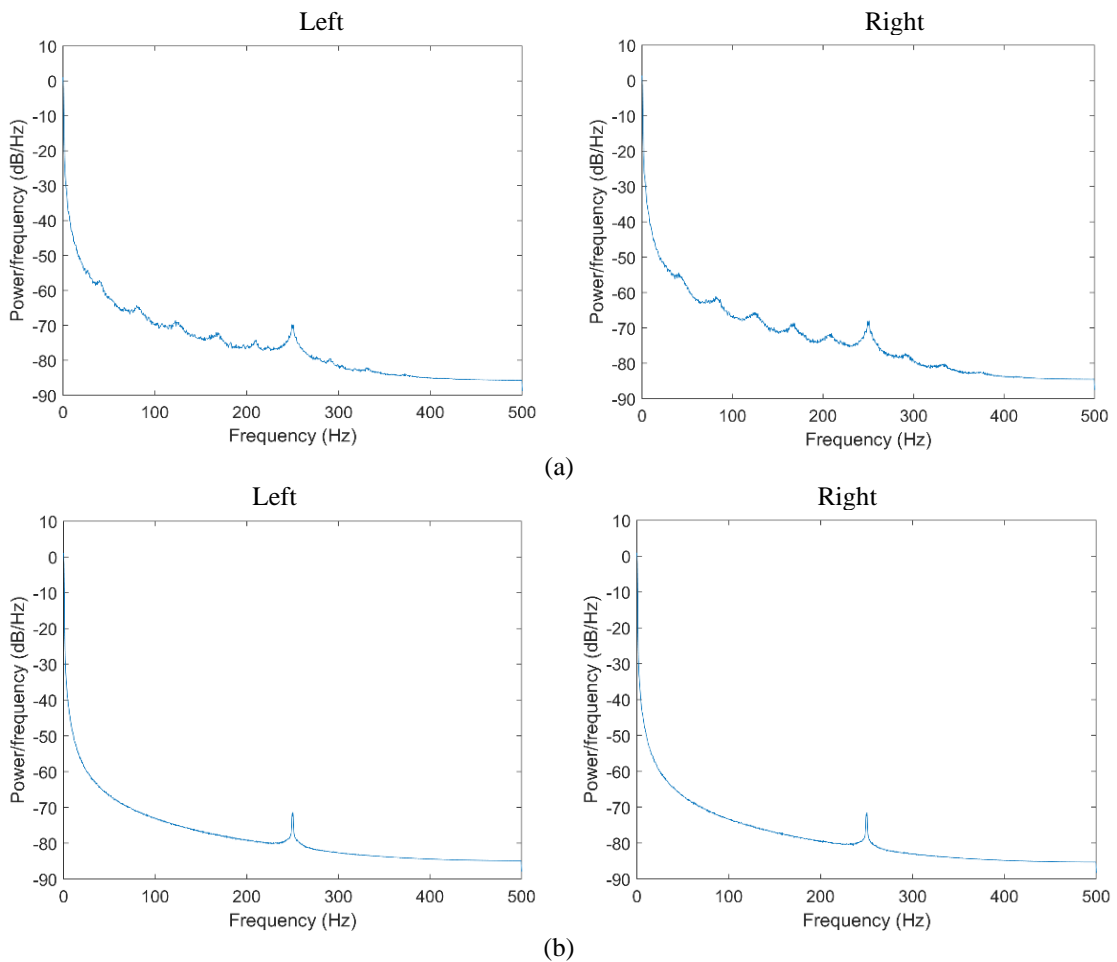


Figure 11. Left and right pupil diameter signals after Welch's periodogram (a) for depressed subject and (b) for normal subject

2.3.6. CNNs

In this study, we delve into the effectiveness of three widely acclaimed pre-trained models - namely, AlexNet, GoogLeNet, and SqueezeNet - for the purpose of depression classification. The dataset employed

for our investigation has been partitioned, allocating 90% for training and the remaining 10% for validation. This partitioning has been executed across distinct data modalities, specifically focusing on the right pupil diameter, left pupil diameter, and a fusion of both pupil diameters.

AlexNet, GoogLeNet, and SqueezeNet are all CNN architectures used for various computer vision tasks, including image and signal classification. Each architecture has its own unique features and design principles:

- AlexNet, a pioneering deep learning architecture by Krizhevsky, Sutskever, and Hinton in 2012, popularized CNNs for image classification. It won ILSVRC with innovations like ReLU activation, dropout, and stacked convolutional and pooling layers in this 5-convolutional, 3-fully connected structure. It consists of eight layers: five convolutional layers followed by max-pooling layers, and then three fully connected layers. The activation function used is the rectified linear unit (ReLU).
- GoogLeNet (Inception-v1), created by Google in 2014, uses “inception” modules for local and global feature extraction. It stacks these modules, ending with fully connected layers. It uses 1×1 convolutions to reduce the number of inputs channels and employs a fire module that combines both 1×1 and 3×3 convolutions.
- SqueezeNet, a 2016 lightweight CNN, uses “fire” modules for efficient spatial and channel-wise info capture. It’s well-suited for resource-constrained devices with fewer parameters in this structure. It utilizes multiple filter sizes (1×1, 3×3, 5×5) within the same layer. It is a deep network but with computational efficiency due to the use of global average pooling and 1×1 convolutions to reduce dimensions.

Pre-trained models have garnered substantial attention within the realm of deep learning due to their proficiency in harnessing expansive datasets and intricate architectures designed to capture intricate high-level features. The trio of models under scrutiny, namely AlexNet noted for its transformative impact on image classification, GoogLeNet boasting its inception module, and SqueezeNet lauded for its computational efficiency, collectively present a diverse spectrum of architectures and methodologies. Through the application of these models, the core objective of this study is to investigate their individual merits and shortcomings, alongside their comprehensive performance across diverse datasets.

By conducting a thorough evaluation encompassing accuracy, computational efficiency, and generalization capabilities, we aim to illuminate the pragmatic implications of employing these pre-trained models for the task of depression classification. It is noteworthy that prior to commencing training, the data undergoes resizing to align with the prerequisites of pre-trained models. Additionally, the classification layer is suitably adjusted to accommodate the binary classification of depressed and healthy classes.

3. RESULTS AND DISCUSSION

The accuracy outcomes resulting from the application of the GoogLeNet model on the left eye dataset stand at 83.33%. On the right eye dataset, the accuracy achieved is 66.67%, while the combined eye dataset yields an accuracy of 83.33%. Upon implementing the SqueezeNet model, the left eye dataset produces an accuracy of 66.67%. The right eye dataset demonstrates an identical accuracy of 66.67%, and for the combined eye dataset, the accuracy rate drops slightly to 58.33%.

When the AlexNet model is employed, the left eye dataset and the right eye dataset both attain a matching accuracy of 83.33%. However, in the case of the combined eye dataset, the accuracy rate slightly decreases to 66.67%. These results are systematically presented in Table 2, offering a comprehensive overview of the accuracy metrics derived from the application of each model on the respective datasets.

Figure 12 illustrates the highest achieved accuracies for each model on different eye datasets. Notably, both GoogLeNet and AlexNet reached a peak accuracy of 83.33% for the left eye dataset. Similarly, AlexNet secured the highest accuracy of 83.33% on the right eye dataset. For the combined eye dataset, the top accuracy of 83.33% was attained using GoogLeNet.

Table 2. Results before segmentation

No.	Data	Healthy	Depressed	GoogLeNet	SqueezeNet	AlexNet
	Left eye dataset	29	29	83.33%	66.67%	83.33%
	Right eye dataset	29	29	66.67%	66.67%	83.33%
	Combined eye dataset	58	58	83.33%	58.33%	66.67%

When assessing accuracy across models, it’s evident that both GoogLeNet and AlexNet consistently outperformed SqueezeNet across all three eye datasets. Thus, these two models are recommended for prioritization in depression-related work involving eye datasets. The accuracy achieved using GoogLeNet and AlexNet on the combined eye dataset remains consistently high, standing at 83.33% for both models.

This suggests that amalgamating data from both eyes yields valuable insights for tasks linked to eye data. Considering the left and right eye datasets, their accuracies are generally comparable across all three models. However, it's noteworthy that AlexNet consistently exhibits the highest accuracy on the right eye dataset (83.33%), indicating its suitability for right eye data analysis.

After segmentation, the accuracy outcomes vary. Specifically, applying GoogLeNet on the left eye dataset results in an accuracy of 60.71%, while the right eye dataset achieves an accuracy of 71.43%. The combined eye dataset exhibits an accuracy of 63.79% for GoogLeNet. For SqueezeNet, the left eye dataset attains an accuracy of 60.71%, the right eye dataset reaches 64.29% accuracy, and the combined eye dataset achieves a notably higher accuracy of 81.03%. Lastly, when utilizing AlexNet, the left eye dataset achieves an accuracy of 78.57%, the right eye dataset secures 67% accuracy, and the combined eye dataset achieves an impressive accuracy of 98.28%. A detailed summary of these results is systematically presented in Table 3, offering a clear overview of the accuracy metrics achieved for each model across the various eye datasets, both before and after segmentation.

Figure 13 provides a visual depiction of the highest accuracy achievements for each model across different eye datasets. Specifically, the highest accuracy attained for the left eye dataset was 78.57% using AlexNet. Likewise, the right eye dataset exhibited its highest accuracy of 71.43% with GoogLeNet. Remarkably, the combined eye dataset achieved the pinnacle accuracy of 98.28%, utilizing the AlexNet model.

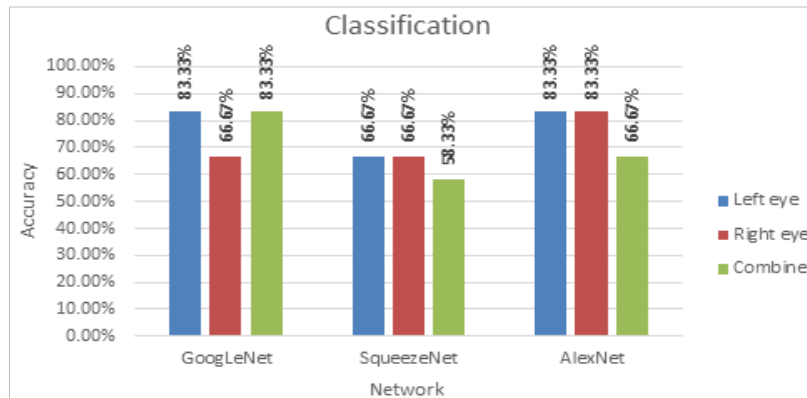


Figure 12. Classification bar chart before segmentation

Table 3. Results after segmentation

No.	Data	Healthy	Depressed	GoogLeNet	SqueezeNet	AlexNet
1	Left eye dataset	29	29	60.71%	60.71%	78.57%
2	Right eye dataset	29	29	71.43%	64.29%	67%
3	Combined eye dataset	58	58	63.79%	81.03%	98.28%

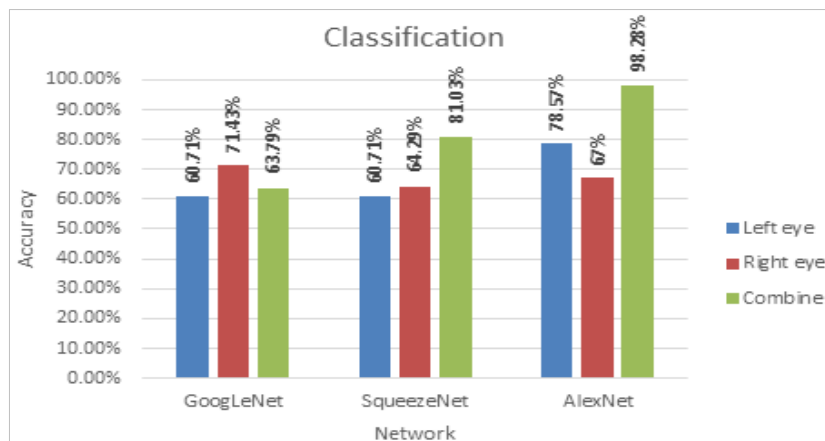


Figure 13. Classification bar chart after segmentation

Upon evaluating the performance of GoogLeNet, SqueezeNet, and AlexNet, it's evident that AlexNet consistently outperformed the others. This is especially noticeable with its higher accuracies on both the left eye dataset and the combined eye dataset. This consistency reinforces the predictive strength of AlexNet for tasks related to eye data. As a result, it's recommended to prioritize the utilization of AlexNet when dealing with these types of datasets.

Notably, the combined eye dataset consistently yielded superior accuracies in comparison to the individual left and right eye datasets across all three models. This observation underscores the potential benefits of aggregating data from both eyes, which can enhance the overall information and potentially elevate the model's accuracy. Therefore, whenever feasible, working with combined eye datasets is advised for eye-related analysis and modeling endeavors. While SqueezeNet didn't achieve the highest accuracy on any individual dataset, its competitive performance is noteworthy, particularly on the combined eye dataset. This suggests that SqueezeNet can serve as a viable alternative, especially when computational resources or model size is a concern. However, if the primary objective is to maximize accuracy and resources permit, AlexNet remains the recommended choice.

Furthermore, the application of segmentation has led to accuracy improvements across different datasets and models. In certain instances, these improvements are substantial, such as the case of SqueezeNet on the combined eye dataset and AlexNet on the combined eye dataset. This underscores the potential benefits of segmenting data to enhance model performance and accuracy.

In Figure 14, the training progress for the combined dataset after segmentation on the AlexNet model is depicted. The following descriptions provide insight into the different curves presented in the figure:

- Training accuracy curve: tracks the accuracy of classifying training examples over iterations/epochs, revealing how well the model performs on the training data.
- Validation accuracy curve: shows the accuracy of classifying validation data during training, indicating the model's ability to generalize. A rising curve signifies effective learning.
- Training loss curve: displays the loss function value during training, quantifying how well the model minimizes prediction errors. A decreasing curve reflects performance improvement.
- Validation loss curve: depicts the loss on a separate validation dataset, helping assess overfitting. A stable or decreasing curve indicates the model's capacity to generalize to new data.

These curves together provide a comprehensive view of the model's training and validation dynamics, enabling insights into its accuracy, generalization ability, and learning progress. Monitoring these curves aids in fine-tuning the model, detecting overfitting, and ensuring its effective application to new datasets. The results suggest that the suggested methodology has important practical implications for enhancing the early identification of MDD where:

- A quasi-objective diagnostic technique using a deep convolutional neural network aids doctors in identifying and monitoring clinical depression. Depression diagnosis, which relies on self-report and physician judgement, may benefit from objectivity. The research implies that binary classification between depressed and healthy people can improve diagnostic accuracy. Accurate and reliable diagnostic equipment reduces false diagnoses and speeds up medical decision-making.
- Enhancing the preprocessing of pupil data signals enhances the effectiveness of the diagnostic system. Deep neural networks excel in signal separation and depression identification, making them viable for therapeutic applications. Data augmentation, particularly the segmentation of each case's signal into five segments, is beneficial when working with a small dataset. This approach increases the size of the dataset, perhaps improving the robustness and ability of the diagnostic system to apply its knowledge to new cases.
- The user's text is a bullet point. The absence of substantial differences in ocular diameter abnormalities, along with their higher frequency in individuals with depression, suggests the presence of a biomarker. This measure has the potential to accurately identify depression, offering a novel approach to understand and assess symptoms of depression.
- The user's text is a bullet point. The study demonstrates that AlexNet surpasses SqueezeNet and GoogLeNet, providing valuable guidance for selecting deep learning models in similar circumstances. Medical practitioners may employ this information to choose models that demonstrate superior performance on aggregated eye datasets. The study's emphasis on enhancing and perfecting the deep learning models demonstrates its commitment to advancement. These findings suggest that doing more research might enhance the performance of the model and increase the capabilities of the diagnostic system. Integrating data from both eyes might enhance depression detection in future studies and system development. This integration has the potential to enhance the assessment of depressed condition by amalgamating data from several sources.

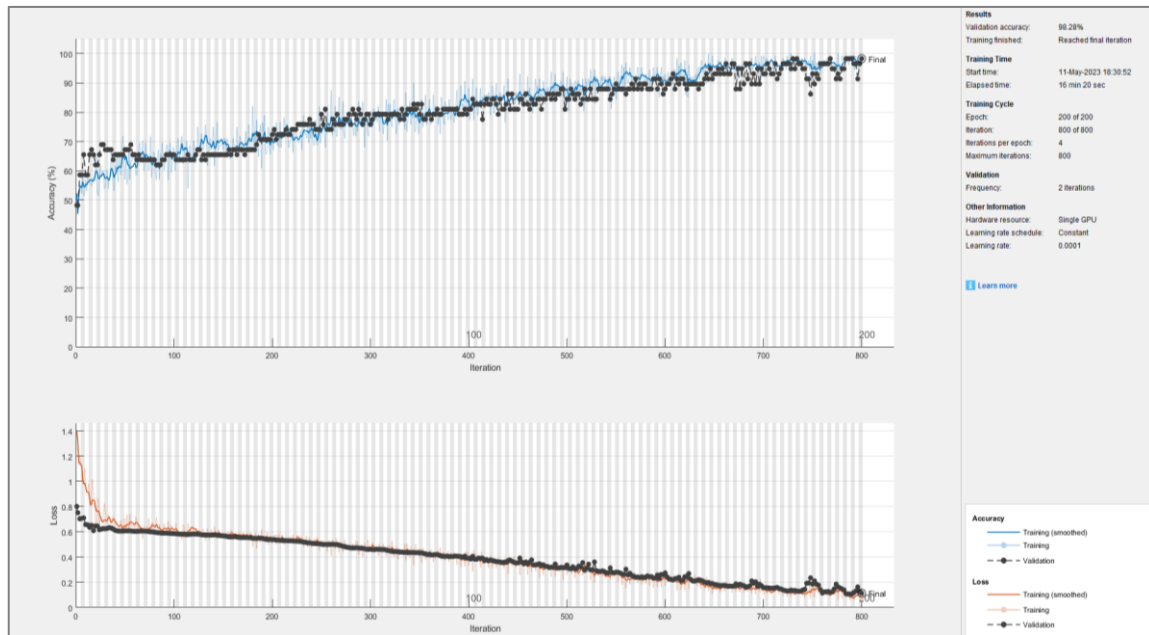


Figure 14. Training progress for combined dataset after segmentation on AlexNet

4. CONCLUSION AND FUTURE WORK

Depression is a highly impactful mental disorder that affects individuals, their social circles, and society at large. Despite available treatment options, diagnosing depression remains challenging due to its subjective nature, relying on self-report and clinical judgment. This study aimed to address this issue by developing a quasi-objective diagnostic system using a DCNN to analyze changes in pupil diameter. The goal was to create a tool to support clinicians in diagnosing and monitoring clinical depression. The study involved a binary classification task, employing the DCNN to differentiate between individuals with depression and those without. Rigorous efforts were invested in refining signal preprocessing techniques for eye data, enabling effective separation and diagnosis of depression and other conditions through deep neural networks. As the dataset was relatively small in size, we went for data augmentation by segmenting each case's signal into five segments. This segmentation procedure has effectively augmented the dataset. Interestingly, while changes in eye diameter did not exhibit significant differences between depressed and healthy individuals, the study noted that the average frequency of these changes was more prominent among depression cases. This observation suggests the potential utility of this metric as a reliable indicator for objectively assessing depression.

In conclusion, the study's findings underscored the superior performance of GoogLeNet and AlexNet compared to SqueezeNet, particularly when applied to combined eye datasets. Future research endeavors should focus on further enhancing and fine-tuning these models. Additionally, the study suggests the potential benefits of integrating data from both eyes for even greater accuracy in depression diagnosis. Ultimately, the developed diagnostic system holds promise for facilitating more objective and accurate assessments of depression, contributing to improved patient care and well-being. The recent advancements have improved the accuracy of measuring pupil diameter. However, acquiring resting state records remains challenging due to potential influences such as light, sound, and uncontrollable eye blinking, which can distort pupil size measurements, complicating accurate interpretation.

Exploring future research directions in contributing to the development of a more robust and embedded system for mental health monitoring, including a wider range of conditions and providing a comprehensive understanding of depression severity involves several key areas. Firstly, there is a need to integrate additional physiological markers, such as heart rate variability, electrodermal activity, or sleep patterns, to enhance the system's understanding of mental health. Investigating how combinations of these markers can offer a more comprehensive insight into individuals' mental well-being is crucial. Secondly, extending the system to detect and classify other mental health conditions beyond depression, like anxiety disorders or stress, requires researching relevant physiological markers and behavioral patterns. Additionally, transitioning from binary to multi-class classification for depression severity and exploring the correlation between severity levels and specific physiological markers can improve the system's accuracy. Longitudinal

studies are necessary to assess the system's performance over time, considering mental health's dynamic nature, while real-world validation with mental health professionals' collaboration ensures its effectiveness and continuous improvement. Evaluating user experience and addressing ethical considerations, including data privacy and responsible technology use, are vital aspects. Finally, optimizing machine learning models using advanced techniques can enhance classification accuracy and generalization.

ACKNOWLEDGEMENTS

The authors express their sincere gratitude to Prof. Karl Jürgen Bär and Prof. Andy Schumann (Jena University Hospital, Department of Psychiatry and Psychotherapy, Jena, Germany) for sharing the dataset which were used in this study and their helpful support. Also, authors would like to thank (Biomedical Engineering Department, Faculty of Engineering, Misr University for Science and Technology, Egypt) for any advice or discussion that improved the study, as well as providing guidance throughout this work.




REFERENCES

- [1] K. J. Bär, W. Greiner, T. Jochum, M. Friedrich, G. Wagner, and H. Sauer, "The influence of major depression and its treatment on heart rate variability and pupillary light reflex parameters," *Journal of Affective Disorders*, vol. 82, no. 2, pp. 245–252, Oct. 2004, doi: 10.1016/j.jad.2003.12.016.
- [2] R. Egg, B. Högl, S. Glatzl, R. Beer, and T. Berger, "Autonomic instability, as measured by pupillary unrest, is not associated with multiple sclerosis fatigue severity," *Multiple Sclerosis*, vol. 8, no. 3, pp. 256–260, Jun. 2002, doi: 10.1191/1352458502ms793oa.
- [3] S. Sirois and J. Brisson, "Pupillometry," *Wiley Interdisciplinary Reviews: Cognitive Science*, vol. 5, no. 6, pp. 679–692, Nov. 2014, doi: 10.1002/wcs.1323.
- [4] M. M. Bradley, L. Miccoli, M. A. Escrig, and P. J. Lang, "The pupil as a measure of emotional arousal and autonomic activation," *Psychophysiology*, vol. 45, no. 4, pp. 602–607, Jul. 2008, doi: 10.1111/j.1469-8986.2008.00654.x.
- [5] T. Partala and V. Surakka, "Pupil size variation as an indication of affective processing," *International Journal of Human Computer Studies*, vol. 59, no. 1–2, pp. 185–198, Jul. 2003, doi: 10.1016/S1071-5819(03)00017-X.
- [6] B. Gingras, M. M. Marin, E. Puig-Waldmüller, and W. T. Fitch, "The eye is listening: Music-induced arousal and individual differences predict pupillary responses," *Frontiers in Human Neuroscience*, vol. 9, no. NOVEMBER, Nov. 2015, doi: 10.3389/fnhum.2015.00619.
- [7] A. Müller, R. Petru, L. Seitz, I. Englmann, and P. Angerer, "The relation of cognitive load and pupillary unrest," *International Archives of Occupational and Environmental Health*, vol. 84, no. 5, pp. 561–567, Jun. 2011, doi: 10.1007/s00420-010-0590-7.
- [8] H. Lüdtke, B. Wilhelm, M. Adler, F. Schaeffel, and H. Wilhelm, "Mathematical procedures in data recording and processing of pupillary fatigue waves," *Vision Research*, vol. 38, no. 19, pp. 2889–2896, Oct. 1998, doi: 10.1016/S0042-6989(98)00081-9.
- [9] B. Hosseinfard, M. H. Moradi, and R. Rostami, "Classifying depression patients and normal subjects using machine learning techniques and nonlinear features from EEG signal," *Computer Methods and Programs in Biomedicine*, vol. 109, no. 3, pp. 339–345, Mar. 2013, doi: 10.1016/j.cmpb.2012.10.008.
- [10] G. J. Siegle, S. R. Steinhauer, V. A. Stenger, R. Konecky, and C. S. Carter, "Use of concurrent pupil dilation assessment to inform interpretation and analysis of fMRI data," *NeuroImage*, vol. 20, no. 1, pp. 114–124, Sep. 2003, doi: 10.1016/S1053-8119(03)00298-2.
- [11] A. Schumann, C. Kralisch, and K. J. Bär, "Interrelation of cardiovascular dysfunction and pupillary fluctuations in patients with major depression," *Biomedical Engineering / Biomedizinische Technik*, Jan. 2013, doi: 10.1515/bmt-2013-4189.
- [12] M. Li, W. Zhang, B. Hu, J. Kang, Y. Wang, and S. Lu, "Automatic assessment of depression and anxiety through encoding pupil-wave from HCI in VR scenes," *ACM Transactions on Multimedia Computing, Communications and Applications*, vol. 20, no. 2, pp. 1–22, Feb. 2023, doi: 10.1145/3513263.
- [13] X. Ding, X. Yue, R. Zheng, C. Bi, D. Li, and G. Yao, "Classifying major depression patients and healthy controls using EEG, eye tracking and galvanic skin response data," *Journal of Affective Disorders*, vol. 251, pp. 156–161, May 2019, doi: 10.1016/j.jad.2019.03.058.
- [14] W. Mumtaz and A. Qayyum, "A deep learning framework for automatic diagnosis of unipolar depression," *International Journal of Medical Informatics*, vol. 132, p. 103983, Dec. 2019, doi: 10.1016/j.ijmedinf.2019.103983.
- [15] P. Sandheep, S. Vineeth, M. Poulouse, and D. P. Subha, "Performance analysis of deep learning CNN in classification of depression EEG signals," in *IEEE Region 10 Annual International Conference, Proceedings/TENCON*, Oct. 2019, vol. 2019-October, pp. 1339–1344, doi: 10.1109/TENCON.2019.8929254.
- [16] J. Zhu *et al.*, "Mutual information based fusion model (MIBFM): mild depression recognition using EEG and Pupil area signals," *IEEE Transactions on Affective Computing*, vol. 14, no. 3, pp. 2102–2115, Jul. 2023, doi: 10.1109/TAFFC.2022.3171782.
- [17] K. Schultebrucks, V. Yadav, A. Y. Shalev, G. A. Bonanno, and I. R. Galatzer-Levy, "Deep learning-based classification of posttraumatic stress disorder and depression following trauma utilizing visual and auditory markers of arousal and mood," *Psychological Medicine*, vol. 52, no. 5, pp. 957–967, Apr. 2022, doi: 10.1017/S0033291720002718.
- [18] C. Zhu, B. Li, A. Li, and T. Zhu, "Predicting depression from internet behaviors by time-frequency features," in *Proceedings - 2016 IEEE/WIC/ACM International Conference on Web Intelligence, WI 2016*, Oct. 2017, pp. 383–390, doi: 10.1109/WI.2016.0060.
- [19] A. Schumann, C. Kralisch, and K. J. Bär, "Spectral decomposition of pupillary unrest using wavelet entropy," in *Proceedings of the Annual International Conference of the IEEE Engineering in Medicine and Biology Society, EMBS*, Aug. 2015, vol. 2015-November, pp. 6154–6157, doi: 10.1109/EMBS.2015.7319797.
- [20] K. Kramarić *et al.*, "Heart rate asymmetry as a new marker for neonatal stress," *Biomedical Signal Processing and Control*, vol. 47, pp. 219–223, Jan. 2019, doi: 10.1016/j.bspc.2018.08.027.
- [21] M. Kang, H. Kwon, J. H. Park, S. Kang, and Y. Lee, "Deep-asymmetry: asymmetry matrix image for deep learning method in pre-screening depression," *Sensors (Switzerland)*, vol. 20, no. 22, pp. 1–12, Nov. 2020, doi: 10.3390/s20226526.
- [22] P. Kowalski and R. Smyk, "Review and comparison of smoothing algorithms for one-dimensional data noise reduction," in *2018 International Interdisciplinary PhD Workshop, IIPHDW 2018*, May 2018, pp. 277–281, doi: 10.1109/IIPHDW.2018.8388373.
- [23] The MathWorks Inc., "Polyfit Documentation," *Natick*, 2023. <https://www.mathworks.com/help/matlab/ref/polyfit.html>.




- [24] The MathWorks Inc., "Polyval Documentation," *Natick*, 2023. <https://www.mathworks.com/help/matlab/ref/polyval.html>.
 [25] J. Smith, "Hamming Window," *Spectral Audio Signal Processing*, 2011. https://ccrma.stanford.edu/~jos/sasp/Hamming_Window.html.

BIOGRAPHIES OF AUTHORS






Islam Ismail Mohamed    is a Teaching Assistant in the Biomedical Engineering Department at the Higher Technological Institute 10th of Ramadan, Egypt. With a B.Sc. in Biomedical Engineering from the Higher Technological Institute in 2009 and a M.Sc. in Control Systems from Cairo University in 2016. Her specialization lies in machine and deep learning, and passionate about integrating technology with healthcare. She can be contacted at email: bioeng.islam@gmail.com.






Mohamed Tarek El-Wakad    is currently a Professor and Vice Dean student's affairs at Faculty of Engineering and Technology, Future University in Egypt (FUE), Cairo, Egypt. Prof. El-Wakad Received the B.Sc. from Helwan University Cairo Egypt, in Mechanical Eng. 1975, the M.Sc. from George Washington University (GWU), DC, USA in medical Eng. 1981, and the Ph.D. from Rensselaer Polytechnic Institute (RPI), Troy, NY, USA in Biomed. Eng 1988. He served in several administrative and academic positions from 1977- now in Helwan Univ., Future Univ. Egypt (FUE), King Saud Univ. (KSU), British Univ. Egypt (BUE), American Univ. Cairo (AUC), and Misr Univ. for Science and Technology (MUST). He can be contacted at email: mohamed.elwakad@fue.edu.eg.






Khaled Abbas Shafie    is a Lecturer in Electrical Engineering Since 2000 until now at the Higher Technological Institute 10th of Ramadan, Egypt. With a B.Sc. from Ain Shams University, a Ph.D. and M.Sc. in Communication Engineering from Cairo University, and his interest lies in logic design and VLSI design. He can be contacted at email: khaled.abbas@hti.edu.eg.



Mohamed A. Aboamer    obtained a bachelor's degree in biomedical engineering in 2004 and a master's degree in the same field in 2009. He earned a doctorate in biomedical engineering from Cairo University's Faculty of Engineering in 2014. He got a Canadian Educational Credential for a Ph.D. degree from World Educational Service on February 19, 2020 (Ref#: 3811222 IMM). In addition, he obtained a Biomedical Engineering consultant number 19157660 from the Saudi Commission for Health Specialties in 2022. He is currently working as an Associate Professor in the Department of Medical Equipment Technology at Majmaah University. His current profession focuses on biomechanics and biomaterials research. He can be contacted at email: m.aboamer@mu.edu.sa.



Nader A. Rahman Mohamed    (Ph.D. in system and biomedical engineering) was born in Egypt in 1973. He received the B.S. and M.S. degrees in Systems and Biomedical Engineering from Faculty of Engineering- Cairo University in June 1996 and June 2002, respectively. He received the Ph.D. degree in Systems and Biomedical Engineering from Faculty of Engineering Cairo University in June 2009. He worked as a biomedical engineering consultant in the field of ophthalmology, medical lasers, and endoscopy in center for advanced software and biomedical engineering consultation (CASBEC), Faculty of Engineering, Cairo University. He joined the department of Biomedical Engineering Faculty of Engineering Misr University for Science and Technology, in September 2009. His current research interests include image and signal processing, artificial intelligence, neural network, biomedical equipment design and control, biomechanics and biomaterials. He can be contacted at email: nader.shaaban@must.edu.eg.